ISSN 2435-5453

Technical Journal of Advanced Mobility

次世代移動体技術誌

巻 頭 言

レ タ ー

JUADA
Japan UAS Industrial Development Association

Vol. 6
2025

進化を続けるジャーナル

テクニカルジャーナル編集委員長
一般社団法人日本 UAS 産業振興協議会
常務理事　岩田　拡也

2025 年がスタート致しました。謹んで新年のご挨拶を申し上げます。

一般社団法人日本 UAS 産業振興協議会（JUIDA）が発行するテクニカルジャーナルは，ドローン産業の振興に役立つ技術情報を産業界の皆様に提供するために創設されたオンライン技術情報誌で，掲載論文は年々増加を続けておりますとともに，ジャーナル自体も進化を続けております。例えば，昨年 2024 年は，技術情報の速報性を向上するため Letter 制度を新設致しました。その結果，大学等の研究室からの速報性の高い論文の投稿が増加致しました。Japan Drone 展でのポスターセッションに大学の研究室から出展し，大学院に進んで論文にまとめ本誌に投稿頂いた例もございました。また，ベンチャーや中小企業の皆様からも論文を投稿頂き，採録となった開発成果をポスターセッションで発表頂いたことで，様々な企業様との連携や商談に繋がった例は，まさに本誌の目指す姿の一つでございます。

今年の Japan Drone2025 でも，本誌のポスターセッションを開催致します。企業やスタートアップの皆様には，実証実験や製品開発，サービスやソリューション創出などで得た先進的な取り組みや知見をご発表いただき，商談に結実する機会として，また日本のみならず世界へ発信する広告としてお役立て頂ければ幸いです。もちろん，大学研究室の若き学生の皆様にも，査読付きの論文となりますので奮ってご参加頂き，研究者としての登竜門として頂ければと存じます。

昨年年始の能登半島の大震災で焼けた街並みと，ウクライナや中東の戦争で焼けた街並みは，よく似ているようで人の絆を伴うか人の憎悪を伴うかの点で対局にありますが，どちらもドローンの活用が促進している点に私達の未来への責任を感じます。JUIDA では，人の絆を伴う前者の災害支援とドローンの関係強化に向けて最大限の取り組みを行っているところです。本誌も，防災とドローンを組み合わせた特集号等を企画することにより，ドローンの技術情報を社会に役立てることができないか模索していきたいと考えております。

ドローンをこのように活用したら現場で役立った，ドローンと何かを組み合わせることで問題を解決できたといった技術情報や実例が多く投稿され，様々な方面に共有されることで本誌も社会や世界に貢献できます。現場で役立ちそうなドローンに関する情報がございましたら，是非奮ってご投稿ください。その一歩一歩の積み重ねが，やがて人々の憎悪の連鎖を断ち切るドローンの活用と，人々の絆を結ぶドローンの活用を生み育てることになると JUIDA は信じます。本年も何卒宜しくお願い申し上げます。

2025 年 1 月吉日

常務理事
岩田　拡也/Kakuya Iwata
産業技術総合研究所 主任研究員。1998 年通商産業省工業技術院電子技術総合研究所に入所。第 16 回電子材料シンポジウム EMS 賞受賞，第 12 回応用物理学会講演奨励賞受賞。白色 LED 開発にてゼロから 1 兆円産業に成長する過程を経験。半導体製造装置開発からロボット技術に目覚め，2004 年に独立行政法人産業技術総合研究所知能システム研究部門に移籍，無人航空機の研究開発をスタート。2007 年日本機械学会交通・物流部門優秀講演表彰を受賞。2008 年に経済産業省製造産業局産業機械課にてロボット政策に従事。2009 年以降「NIIGATA SKY PROJECT」の無人航空機開発を立ち上げる。

Letter

脳波計測によるストレス解析のための実機とCGのドローンにおけるディスクレパンシー評価

草野　智[*1]，福原　悠介[*2]，原　進[*3]，満倉　靖恵[*4]，上出　寛子[*5]
名古屋大学大学院工学研究科機械システム工学専攻[*1]
名古屋大学工学部機械・航空宇宙工学科[*2]
名古屋大学大学院工学研究科航空宇宙工学専攻[*3]
慶應義塾大学理工学部システムデザイン工学科[*4]
京都大学大学院法学研究科[*5]

近年，Urban Air Mobility（UAM）に関する技術が世界中で研究されている一方，UAMやドローンの社会受容性については十分に検討されていない。そこで著者らが所属する研究グループでは，アンケートによる主観評価と簡易脳波計測にもとづく感性アナライザによる客観評価を組み合わせた社会受容性評価手法を提案した。この手法の有効性は確認されている。2023年12月に実施された便益効果評価実験では，UAMの社会受容性を向上させる手法として場面想定が提案された。しかしながら，得られたデータの信頼性が不十分であったため，適切な実験環境が設定できていない可能性，および十分な場面想定ができていない可能性があった。また，参加者がいくら場面想定を十分にできたとしても，実際のUAMとCGとの乖離は無視し難い。そのため，実験環境を改善することで，実際のUAMとCGのディスクレパンシー（乖離）を小さくする必要がある。本研究では，実際のUAMを用いた実験は困難であるため，ドローン（マルチコプター）を用いてこの種の検討を行う。本発表では，一般の参加者を対象にするのではなく，著者が所属する研究グループの学生を対象に実施された実験について述べる。

Keywords: ディスクレパンシー，脳波計測，感性アナライザ，社会受容性，ストレス，UAM

Discrepancy Evaluation Between Actual and Computer Graphics Drones for Stress Analysis by EEG Measurement

Satoshi Kusano[*1], Yusuke Fukuhara[*2], Susumu Hara[*3], Yasue Mitsukura[*4], Hiroko Kamide[*5]
Department of Mechanical Systems Engineering, Graduate School of Engineering, Nagoya University[*1]
Department of Mechanical and Aerospace Engineering, School of Engineering, Nagoya University[*2]
Department of Aerospace Engineering, Graduate School of Engineering, Nagoya University[*3]
Department of System Design Engineering, Faculty of Science and Technology, Keio University[*4]
Graduate School of Law, Kyoto University[*5]

Technologies related to urban air mobility (UAM) are being studied worldwide. However, the social acceptance of UAMs and drones has not been investigated thoroughly. To address this issue, the authors propose a social

acceptance evaluation method that combines subjective assessments by questionnaires with objective evaluations using a Kansei Analyzer based on a simple electroencephalograph. The effectiveness of the proposed method was confirmed. In the benefit-effect assessment conducted in December 2023, scene assumption was proposed as a means of improving social acceptance. However, the reliability of the obtained data was insufficient, and there was a possibility of not preparing an appropriate experimental environment or assuming sufficient scenes. Even if the subject is able to adequately assume the scene, it is difficult to ignore the discrepancy between the actual UAM and CG. Therefore, it is necessary to reduce the discrepancy between the actual UAM and CG by improving the experimental environment. As it is difficult to conduct experiments using an actual UAM, in this study, we used a drone (multicopter) for the investigation. This paper presents the results from a preliminary experiment conducted with students in our research group, rather than with participants from the general public.

Keywords: Discrepancy, EEG measurement, Kansei analyzer, Social acceptance, Stress, Urban air mobility

1. Introduction

Drones are now becoming popular, and industrial drones for logistics and urban air mobility (UAM) for mobile infrastructure are being commercialized. Although there is ongoing research and development on the safety and performance of drones, there has been little research on the social acceptance of the aerial industrial revolution [1]. Social acceptance is generally considered in terms of technical, institutional, and market aspects [2]. However, in this study, it refers to the psychological aspects of the extent of noise and fear accepted by the public. In the past, when new infrastructure was introduced, such social acceptance was not considered seriously. As a result, public protests occurred after airports and high-speed railway lines were built. Although it is necessary to reflect on such experiences, the authors are unaware of any specific evaluation metrics for social acceptance evaluation at present. Therefore, to enable the smooth market introduction of UAM, it is necessary to establish an objective evaluation method for social acceptance, set acceptance criteria, and develop UAM based on such criteria. Hara et al. [3] attempted to objectively evaluate social acceptance by measuring stress levels using an analyzer based on simple electroencephalography.

In addition, according to a psychosocial survey on noise by Yamanouchi et al. [4], it was hypothesized that stress tolerance changes with different applications and stakeholders, even for the same mobility. Furthermore, previous studies reduced the subjective stress measured from drone noise to formulate drone flight operation conditions [5]. However, uniformly setting the noise level and developing drones accordingly cannot necessarily improve social acceptance by citizens or users. Therefore, it is necessary to search for an acceptable noise level for each application and stakeholder. However, such research has not yet been conducted [6]. Takahara et al. [7] conducted a benefit-effect evaluation experiment to clarify the acceptable noise level for each use through the scene assumption method. The results of the experiment showed that the acceptable noise level may be higher when using a UAM with a large social impact compared to daily use vehicles for commuting to work. However, the reliability of the obtained data was insufficient. Therefore, it is necessary to improve the experimental environment and investigate the stress factors. Even if the subject is able to adequately envision the scene, the discrepancy between the real UAM and CG is difficult to ignore. Therefore, it is necessary to reduce the discrepancy between the real UAM and CG by improving the experimental environment. As it is difficult to conduct experiments using a real UAM, in this study, we used a drone for the investigation. We used an analyzer

based on simple electroencephalograph (EEG) measurement to evaluate the discrepancy in the stress levels between a real drone and CG drone, and discussed the fundamentals of constructing an experimental environment when using a UAM as a target. In the future, this research aims to contribute to the smooth social implementation of UAM. A preliminary experiment was conducted not with general participants, but with students in the authors' research group. In addition, we summarize the results of a simpler analysis of the preliminary experiment without the weighting described in Section 4-3 in [8].

2. Objective evaluation method using a simple electroencephalograph

Sociopsychological questionnaires are often used to assess emotional changes in social acceptance. However, as these questionnaires are subjective, they cannot accurately capture real-time emotional changes. For the EEG measurement in this study, we employed a Kansei Analyzer (**Figs.1** and **2**) [9] from Dentsu Science Jam Inc., which is a simple EEG-measuring device designed for emotion measurement. The Kansei Analyzer is a simple electroencephalograph designed to measure five emotional states: stress, concentration, preference, calmness, and interest. Its real-time nature makes it useful for time-series sensitivity assessments. In principle, sensitivity index values are estimated from EEG in real time by pattern matching with a database accumulated over many years such that the feature values based on the EEG shapes and sensitivity index values based on biohormone levels match one-to-one. This is based on the correlation between changes in biohormones related to emotional responses and EEG feature patterns (i.e., hormone fluctuations affect EEG patterns and vice versa).

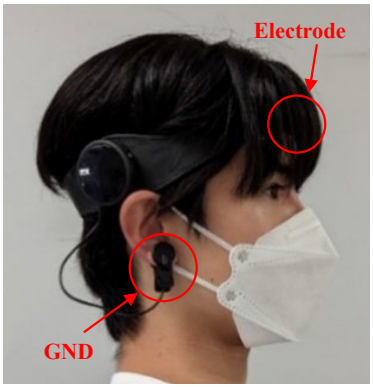

Fig.1　Kansei analyzer.

Fig.2　Installation method.

3. Stress factors given by drones

To evaluate the stress-level discrepancy between an actual drone and a CG drone, it is necessary to create a CG based on the stress factors imparted by drones to people. In this section, we explain the stress factors that drones cause to people based on related studies. First is the noise, which is considered to be the strongest factor in the stress caused by drones. Unlike other environmental noises (e.g., traffic and aircraft noise), drones generate noise that contains many high-frequency components and pure tones [6]. Owing to this characteristic, drone noise is often perceived as more unpleasant than normal environmental noise. The unpleasantness is amplified by the rapid modulation of sound particularly due to the rotation of the propeller. The second factor is the size of the drone. It has been reported that larger drones have a greater visual presence, and seem more intimidating and dangerous [10]. The third factor is flight altitude. Drones flying at lower altitudes are reported to cause greater concerns regarding noise, safety, and privacy invasion [10]. Finally, the flight speed of the drone is also a factor. Sudden changes in direction and flight at high speeds have been reported to cause stress.

Specifically, at a higher speed, it is more difficult to predict the flight of the drone and there is a greater fear of collision [6]. Based on the aforementioned stress factors caused by drones, we focused on the drone size, which are frequently reported stress factors, and evaluated the stress-level discrepancies between actual drones and CG drones.

4. Experimental method

As a preliminary experiment, we did not involve general participants, but explained the details of the experiment to students (6 students in their 20 s) in our research group, and they consented to cooperate in the experiment.

4-1 Experiment environment and flight path

The actual and CG drones are shown in Figs.3 and 4, and the experimental environment and drone flight paths are shown in Figs.5 and 6, respectively. The drone weighed 249 g, measured 298 × 373 × 101 mm, had a maximum flight time of 30 min, and a noise level of 70 dB at the closest approach (0.8 m from the subject).

Next, the flight path of the drone is described. The drone ascended from a platform 0.4 m above the ground to a height of 1.2 m over a period of 5 s, approached the subject over a period of 15 s, and stopped 0.8 m in front of the subject. The subjects' EEG data for 20 s up to this point were measured using a Kansei analyzer. The CG drone was created based on the size, noise level, and flight path of the actual drone.

Fig.3 Actual drone.

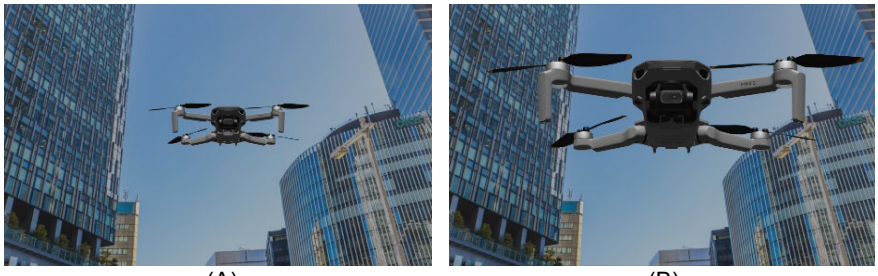

(A) (B)

Fig.4 (A) CG1 drone (Small), (B) CG2 drone (Large).

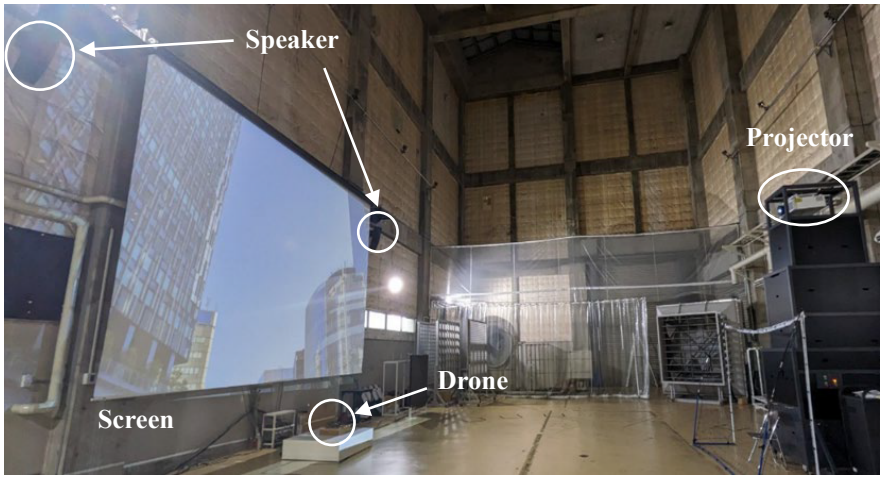

Fig.5 Experiment environment.

4-2 Experimental protocol

The experimental flow is shown in Fig.7. The participants were asked to view three types of drones: an actual drone, a CG1 drone, and a CG2 drone with an interval between them to allow for the questionnaire and rest time. To account for the effect of order, each subject viewed the three types of drones in different orders.

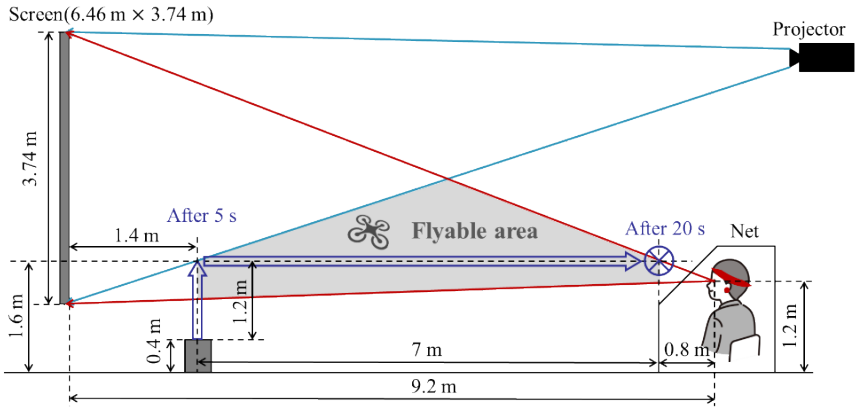

Fig.6　Flight path.

Next, we describe the CG drones. CG1 was a CG-drone that was 2/3 the scale of the real drone, and CG2 was a CG-drone that was 3/2 the scale of the real drone. The CG sounds were recorded from the actual drone flights, processed, and edited. The noise level was measured according to the characteristics of the human ear (characteristic A) [11], which states that human senses become duller for lower loudness and frequency of sound.

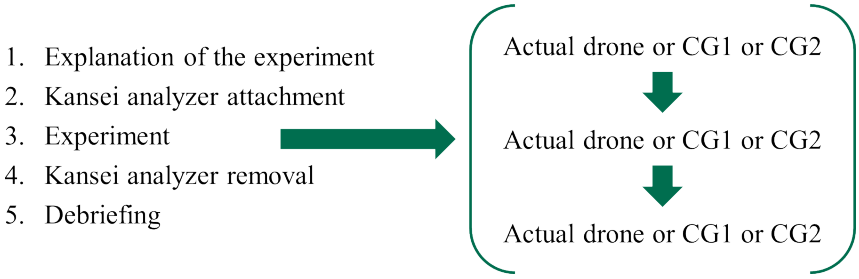

Fig.7　Experimental flow.

4-3　Analysis method

This section describes the analysis method for the stress levels measured using the Kansei analyzer. The discrepancy between the CG drone and real drone was evaluated when the size and noise level of the CG drone were changed. The stress level was measured for 20 s before and after the drone started to fly or when the CG drone started to play its video. The measured data for 20 s before and after the flight were weighted based on the mean and standard deviation of each data point. The data was weighted because it is easier for the stress level to change from 50% to 60% compared to the change from 90% to 100%.

Let us assume a_t as the stress level at time t [s], μ is the mean value, and σ is the standard deviation. Then, the weights w_t are determined according to the following rule.

- $|a_t - \mu| \leq \sigma$, then $w_t = 1$
  - $a_t \rightarrow a_t$
- $\sigma < |a_t - \mu| \leq 2\sigma$, then $w_t = 1.5$
  - $a_t \rightarrow 1.5a_t$
- $2\sigma \leq |a_t - \mu| < 3\sigma$, then $w_t = 2$
  - $a_t \rightarrow 2a_t$
- $3\sigma \leq |a_t - \mu|$, then $w_t = 2.5$
  - $a_t \rightarrow 2.5a_t$

Based on the stress level measured by the Kansei analyzer, the weighted average of the stress level of participant i during the 20 s before and after the start of the flight (or the start of the CG) can be expressed using Eqs. (1) and (2), respectively. Let us assume t_s [s] as the time at which the drone flight starts (or CG starts).

$$\bar{a}_{i,1} = \frac{\sum_{t=t_s-20}^{t_s} w_t a_t}{\sum_{t=t_s-20}^{t_s} w_t} \tag{1}$$

$$\bar{a}_{i,2} = \frac{\sum_{t=t_s}^{t_s+20} w_t a_t}{\sum_{t=t_s}^{t_s+20} w_t} \tag{2}$$

Using Eqs. (1) and (2), the stress variation for drone type j for the i-th participant is expressed by Eq. (3). Note that $j = 0$ is the actual drone, $j = 1$ and $j = 2$ represent CG1 and CG2, respectively.

$$x_i^j = \bar{a}_{i,2} - \bar{a}_{i,1} \ (j = 0, 1, 2) \tag{3}$$

Using Eq. (3), the average variation of drone type j for experimental group k is expressed by Eq. (4), where N_k is the number of participants in each experimental group (A or B).

$$y_k^j = \frac{1}{N_k} \sum_i^{N_k} x_i^j \ (j = 0, 1, 2, k = A, B) \tag{4}$$

Using Eq. (4), the discrepancy value between the actual drone and CG drone in experimental group k is expressed by Eq. (5).

$$D_k^j = \left| y_k^j - y_k^0 \right| (j = 1, 2, k = A, B) \tag{5}$$

In Eq. (5), the drone type with a smaller value is interpreted as having a smaller discrepancy with the real drone. By improving the CG such that D_k^j approaches zero, we can develop a social acceptance simulator to evaluate an appropriate level of stress.

5. Experimental results and discussion

5-1 Experimental results

In this experiment, due to the small number of participants and the focus solely on drone size, only experimental group A is considered. Average stress variation values for all drone types and the distribution of the stress variation shown in **Fig.8** and **Fig.9**, respectively. The deviation values calculated from **Fig.8** are $D_A^1 = 3.18$ and $D_A^2 = 1.04$, indicating that the larger CG drones have smaller deviation values than the smaller CG drones. However, as there is no y_A^0 (actual drone) between y_A^1 (CG1) and y_A^2 (CG2), it is difficult to set the deviation from the actual drone to zero by changing the size of the CG drone. In the distribution of the stress variation for CG1 shown in **Fig.9**, one participant exhibited an unusually high value (16.7%), which significantly influenced the average stress variation value for CG1. According to the questionnaire responses, this participant reported having more frequent interactions with drones in daily life compared to the other participants and indicated feeling no stress toward any of the three drone types viewed during the experiment. Therefore, it is inferred that when viewing CG1, the participant may have experienced heightened stress related to factors other than the drone itself, such as the presence of others or tension in the experimental setting.

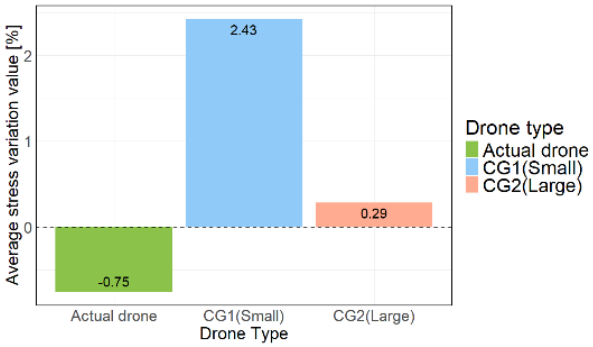

Fig.8 Average stress variation values (N=6).

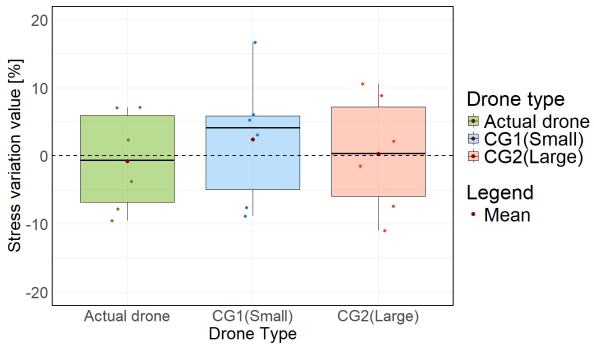

Fig.9 Distribution of the stress variation (N=6).

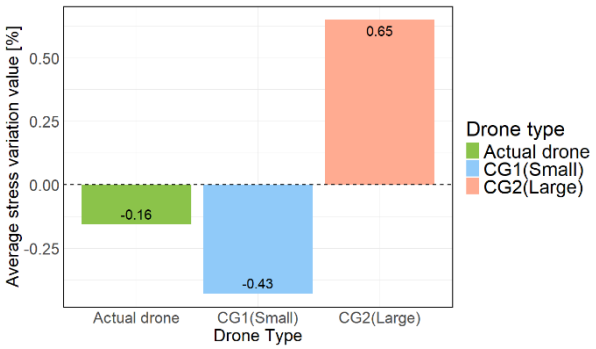

Fig.10 Average stress variation values (N=5).

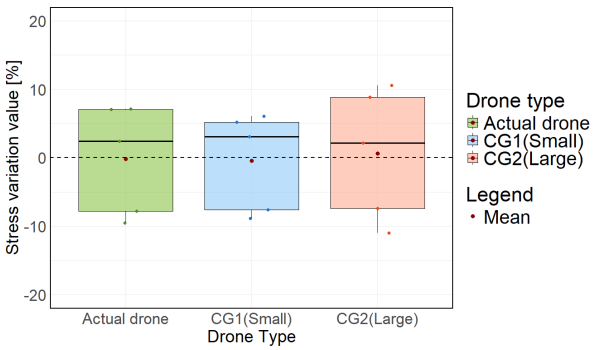

Fig.11 Distribution of the stress variation (N=5).

5-2 Discussion

As mentioned in Section 5-1, the participant who exhibited an unusually high stress change value for CG1 likely experienced significant stress from factors unrelated to the drone itself. Since the primary aim of this experiment is to evaluate the discrepancy between the actual and CG drones based on stress levels, it cannot be confidently stated that the data from this participant, with an extremely high stress variation value for CG1, are entirely reliable. Therefore, Figs.10 and 11 present the average stress variation values and the distribution of stress variation after excluding the data from this participant. The deviation values calculated from Fig.10 are $D_A^1 = 0.27$ and $D_A^2 = 0.81$, indicating that the smaller CG drones have smaller deviation values than the larger CG drones. Furthermore, because y_A^1 (CG1) and y_A^2 (CG2) encompass y_A^0 (actual drone), it is suggested that adjusting the size of the CG drones could bring the deviation value closer to zero. However, because there is no guarantee of a linear relationship between the size of the CG drones and stress levels, the data from Fig.10 only indicates that the average stress variation value for the actual drone lies between those for CG1 and CG2. Therefore, it is necessary to explore methods for reducing the deviation value by conducting experiments with an increased variety of CG drones of different sizes.

In this experiment, the small sample size led to individual participant data significantly influencing the overall results. As shown by comparing Figs.8 and 10, the differences in sample size caused substantial variations in the outcomes. Therefore, we believe that increasing the sample size in future experiments will yield more reliable results, less affected by individual data points. If similar results to those in Fig.10 can be obtained with a larger sample, it may be possible to adjust the size of the CG drone to reduce the deviation from the actual drone. Moreover, if the deviation can be minimized to near zero, it will open the possibility of developing a simulator capable of accurately assessing the stress levels associated with drones.

Contrary to the hypothesis that the average stress variation for an actual drone would be positive, the

experiment produced negative values. This may be due to the fact that many participants were recruited from within the laboratory and were already familiar with drones, leading to a reduced sense of stress. Additionally, it is possible that the stress from the pre-experiment tension exceeded the stress induced by the drone flight.

6. Future prospects

The results of this experiment suggest that it is feasible to design an appropriate experimental environment for researching the social acceptance of next-generation aerial vehicles. These findings indicate that it may be possible to develop an experimental setup to investigate the effects of stress, even with drones replacing flying vehicles. However, the results of this study were significantly influenced by the sample size and the fact that participants were already familiar with drones in their daily lives, which limits the definitive conclusions that can be drawn. In future experiments, we plan to increase the sample size and target individuals unaccustomed to drones in their daily lives. This approach is expected to yield more reliable results than those obtained in this study. Additionally, while this experiment compared the actual drone with CG1, a small-scale CG drone, and CG2, a large-scale CG drone, future studies should include a CG drone of the same size as the actual drone. This would allow an investigation into whether there is any inherent discrepancy in the stress levels between the actual and CG drones. By incorporating a same-size CG drone, researchers could assess not only the presence of discrepancies but also how to adjust the size of CG drones to minimize deviations from the actual drone. Furthermore, evaluating the discrepancies by varying both the size and noise levels of the CG drones could offer new insights and deepen our understanding of the factors influencing the social acceptance of UAM.

Acknowledgment

This work was supported in part by the Amano Institute of Technology.

Received: December 3, 2024
Accepted: December 12, 2024

References

[1] Ministry of Economy, Trade and Industry : “Advanced Air Mobility Roadmap (in Japanese)”, Public-Private Committee for Advanced Air Mobility, 2022.

[2] Matsuoka, S. : “Social Innovation and Regional Sustainability - Fostering Placemaking and Social Acceptance (in Japanese)”, Yuhikaku, 2018.

[3] Hara, S., Mitsukura, Y., and Kamide, H. : “Noise-Induced Stress Assessment —On the Difference Between Questionnaire-Based and EEG Measurement-Based Evaluations—”, *Technical Journal of Advanced Mobility*, Vol. 3-6, pp. 81-90, 2022.

[4] Yamanouchi, K., Hisata, M., and Yamamoto, K. : “A study of psychosocial factors affecting community noise annoyance (in Japanese)”, *Comprehensive Urban Studies*, Vol. 18, pp. 65-87, 1983.

[5] Torija, A. J., and Nicholls, R. K. : “Investigation of Metrics for Assessing Human Response to Drone Noise”, *International Journal of Environmental Research and Public Health*, Vol. 19-6, 3152, 2022.

[6] Shaffer, B., Pieren, R., Heutschi, K., Wunderli, J., and Becker, S. : “Drone Noise Emission Characteristics and Noise Effects on Humans—A Systematic Review”, *International Journal of Environmental Research and Public Health*, Vol.18-11, 5940, 2021.

[7] Takahara, K., Kusano, S., Hara, S., Mitsukura, Y., and Kamide, H. : “Development of Benefit-Effect Assessment Method Using EEG Measurement for Improving Social Acceptance of Urban Air Mobilities”, *Proceedings of the International Council on Electrical Engineering Conference 2024*, O-129, 2024.

[8] Fukuhara, Y., Kusano, S., Hara, S., Mitsukura, Y., and Kamide, H. : “Evaluation of Discrepancy Between Real Flight and CG for Stress Analysis Using EEG Measurement in Drone Flying Environment (in Japanese)”, *Proceedings of the 61st JSASS*

Autumn Joint Conference of Chubu and Kansai Branches, C2, 2024.
[9] Mitsukura, Y., “How Brain Waves Hint at Early Signs of Dementia”, *Nature Portfolio*, 2024.
[10] Bretin, R., Khamis, M., and Cross, E. : ““Do I Run Away?”: Proximity, Stress and Discomfort in Human-Drone Interaction in Real and Virtual Environments”, *Human-Computer Interaction – INTERACT 2023*, Springer, pp. 525–551, 2023.
[11] NTi Audio : “Frequency Weightings for Sound Level Measurements,” https://www.ntiaudio.com/en/support/knowhow/frequency-weightings-for-sound-level-measurements (Accessed : July 29, 2024).

草野　智
2023 年宇都宮大学工学部基盤工学科卒業。同年名古屋大学大学院工学研究科機械システム工学専攻博士前期課程入学，現在に至る。空飛ぶクルマの社会受容性に関する研究に従事。
Satoshi Kusano
Satoshi Kusano received the B.E. degree from the Department of Fundamental Engineering, Faculty of Engineering, Utsunomiya University in 2023. In the same year, he entered the Master’s Program in Mechanical Systems Engineering at the Graduate School of Engineering, Nagoya University. His research interests include social acceptance of UAM.

福原　悠介
2020 年名古屋大学工学部機械・航空宇宙工学科入学。現在，空飛ぶクルマの社会受容性に関する研究に従事。
Yusuke Fukuhara
Yusuke Fukuhara entered the Department of Mechanical and Aerospace Engineering, School of Engineering, Nagoya University in 2020. His research interests include social acceptance of UAM.

原　進
1996 年 9 月慶應義塾大学大学院理工学研究科機械工学専攻後期博士課程修了，博士（工学）。日本学術振興会特別研究員，カリフォルニア大学バークレー校訪問研究員，豊田工業大学工学部助手・助教を経て 2008 年から名古屋大学大学院工学研究科。現在同航空宇宙工学専攻教授。
E-mail : haras@nuae.nagoya-u.ac.jp
Susumu Hara
Susumu Hara received the B.S., M.S., and Ph.D. degrees from Keio University, Japan, in 1992, 1994, and 1996, respectively. In 2000, he joined the faculty of Toyota Technological Institute, Nagoya, Japan. In 2008, he joined the faculty of Nagoya University, Nagoya, Japan, where he is currently a Professor with the Department of Aerospace Engineering.

満倉　靖恵
徳島大学博士（工学），慶應義塾大学博士（医学）。徳島大学助手，岡山大学専任講師を経て 2011 年より慶應義塾大学理工学部准教授，2018 年より同教授。研究テーマは，生体信号解析（脳波，筋電図，EOG，心電図，体温，呼吸，唾液アミラーゼ，NIRS，fMRI），ブレイン・コンピュータ・インターフェース，うつ病，認知症，メディカルバイオマーカー。SfN，IEEE，ARVO 会員。
Yasue Mitsukura
Yasue Mitsukura received the Dr.Eng. degree from the University of Tokushima and the Dr.Med. degree from Keio University, Japan. Since 2011, she has been a Professor with Keio University. Her research interests include bio-signal analysis (EEG, EMG, EOG, ECG, GSR, and body temperature, breath, salivary amylase, NIRS, and fMRI), brain–computer interfaces, Depression, Dementia, and Medical bio-marker. She is a member of SfN, IEE, ARVO.

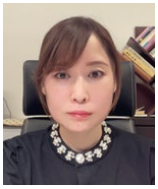

上出　寛子

2008 年大阪大学大学院博士課程修了。博士（人間科学）。2009-2015 年大阪大学大学院基礎工学研究科特任助教。2015-2016 年東北大学電気通信研究所助教。2016-2024 年名古屋大学未来社会創造機構特任准教授。2024 年より京都大学大学院法学研究科特定准教授，現在に至る。HRI, 仏教哲学, 物とのインタラクションに関する研究を行っている。

Hiroko Kamide

Hiroko Kamide completed a Ph.D. in Human Sciences at Osaka University in 2008. From 2009 to 2015, she served as a Specially Appointed Assistant Professor at the Graduate School of Engineering Science, Osaka University. From 2015 to 2016, she held the position of Assistant Professor at the Research Institute of Electrical Communication, Tohoku University. From 2016 to 2024, she served as a Designated Associate Professor at the Institute of Innovation for Future Society, Nagoya University. Since 2024, she has been a Program-Specific Associate Professor at the Graduate School of Law, Kyoto University. Research focuses include Human-Robot Interaction (HRI), Buddhist philosophy, and interaction with objects.

Letter

映像伝送中継局向け固定翼 UAV における旋回半径偏差と機首方位角を用いた高精度旋回経路追従制御技術の研究

三浦　航，安川　慧，上羽　正純
室蘭工業大学大学院

近年，無人航空機（UAV）は，様々なサービスへの利用が広がっている。中でも固定翼 UAV は長時間飛行や広域観測に有利である。固定翼 UAV の利用例の 1 つである，無線中継局を実現するには指定した円経路に沿って正確に旋回し続ける必要がある。そこで，本稿では固定翼 UAV の旋回半径制御系と機首方位角制御系から構成される新たな高精度旋回経路追従制御系を提案し，6 自由度シミュレーションによりその制御系が正常に動作することを確認するとともに，さらに飛行実証を行った結果を報告する。

Keywords: 固定翼 UAV，旋回，ロール角，方位角，飛行実証

Highly Accurate Turn Path Tracking Control Technology for Fixed-wing UAV Using Radius Deviation and Nose Heading Angle to Realize Video Transmission Relay Station

Wataru Miura, Kei Yasukawa, Masazumi Ueba
Graduate School of Muroran Institute of Technology

Unmanned Aerial Vehicles (UAV) have recently been used to provide many kinds of services, among them fixed-wing UAVs are advantageous for long flights and wide-area observations. In order to realize wireless relays station by the UAV, the UAV should continue to accurately turn along a predetermined circular path with its radius specified. To realize the path, we propose a new turn path control system that consists of radius deviation control and nose heading angle control on the UAV, and describe simulation results by which it is confirmed that the proposed control system worked well. And finally, we describe results of the flight verification experiment.

Keywords: Fixed-wing UAV, turning, roll angle, yaw, Flight verification

1. Introduction

In recent years, the use of unmanned aerial vehicles has advanced, and research and development are underway to provide future services in the fields of agriculture and forestry, such as crop pest control, farmland monitoring, surveying disaster areas, terrain measurement, transporting supplies, and radio relay for securing communication

links [1]. In this situation, we have proposed a video transmission relay system using a fixed-wing UAV as a relay station, as shown in Fig.1. Currently, multi-copters, which are rotary-wing UAVs, are often used for observation. On the other hand, fixed-wing UAVs are more advantageous when observing large areas over long distances in a short period because they have a long endurance. Focusing on its long endurance, fixed-wing UAVs can be used as a wireless relay station for the video transmission relay system by making it turn along a predetermined circle path accurately and continuously. There are many papers on turning techniques. For example, in paper [2], flexible path following is essential when fixed-wing UAVs are used for various missions such as surveillance and disaster applications, so they aimed to follow complex paths, including curves, and confirmed their performance through both simulations and flight experiments. Also, in paper [3], a method is proposed to generate a turning path for a fixed-wing UAV without sacrificing maneuverability and safety, with the goal of enabling the fixed-wing UAV to safely perform its mission in a confined space. Also, in paper [4], a control method for rapid direction change is proposed for the purpose of carrying out missions such as surveillance and search and rescue without compromising the advantages of fixed-wing UAVs, such as high speed. However, none of them describe how to make the UAV turn along the predetermined circular path accurately and continuously.

Therefore, we propose a new turn path tracking control system that makes use of the target nose heading angle and turning radius. By using the control system, at first, computer simulations were carried out for small fixed-wing UAV so as to confirm its validity. Then, flight experiment was conducted to verify the control system.

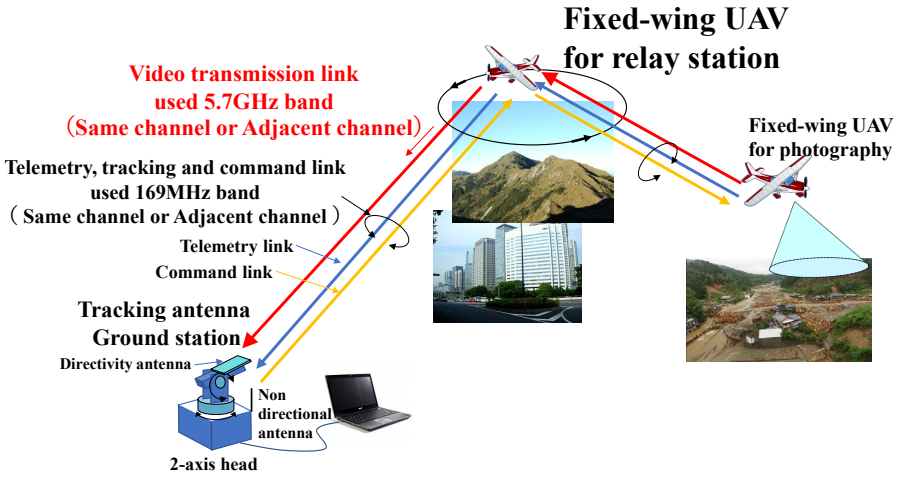

Fig.1 Image of video transmission relay system using fixed-wing UAVs.

2. Conventional turn path control and problems

The authors aimed at achieving highly accurate turn path tracking by using two control systems. One is a roll angle control system focusing on lateral force balancing by aileron operation. The other is a turn radius control system of which rudder command is given by the difference between the target turn path radius and the actual turn radius [6]. After confirming the validity of the method by computer simulation, the flight experiment was carried out as shown in Fig.2. The red line shows the turning trajectory, which deviates significantly from the target path shown in black. The reason is that as the roll angle control system and the turning radius control system were designed independently, when the vehicle deviates significantly from the target turn path, the force generated by the roll angle control system offset the force generated by the turn radius control. That is to say, when the UAV is located inside the target turn path, the force by the roll angle of which radius path is cancelled out by the force of the rudder angle, resulting in the turn radius which is larger than that of the target turn path.

In the same way, when the UAV is located outside the target turn path, the force generated by the rudder is added to the force generated by the roll angle, therefore, that results in a small turn path.

In addition, even though the simulation was successful in turning in the method we proposed [6], the successful accurate turning could not be reproduced in the flight verification experiment. We confirmed that this is due to the expansion of the initial deviation caused by the delay in the control system that occurs immediately after the start of the turn. In fact, simulations performed with our methods, do not take initial deviations into account. Therefore, this time, the proposed methods simulations including initial deviations we carried out to confirm convergence.

From above results, it is clarified that it was necessary to consider the balance adjustment between the roll angle control system and the turning radius control system which uses the rudder. Before investigating the method to design the balance adjustment, we explored to realize a highly accurate turn path tracking system by only roll angle control system based using deviation of both turn radius and heading angle.

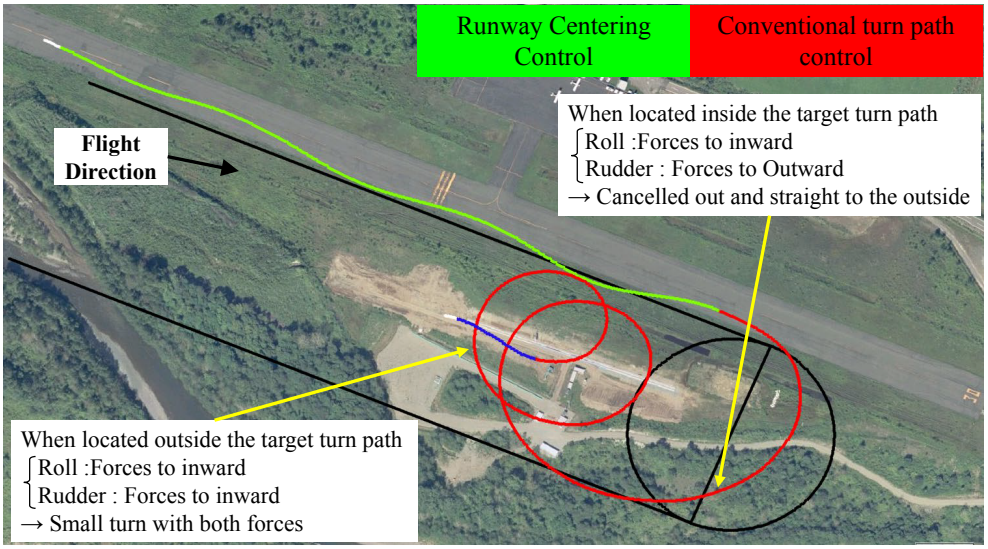

Fig.2　Flight experiment at shiraoi gliding port by conventional turn path control [6] technology.

3. Proposal of highly accurate turn path tracking control method

3-1 Control system policy and configuration

We propose a new control system to track the turning path accurately, which consists of a turn radius control system and a nose heading angle control system. Both control systems use the roll angle control system. The commands to the nose heading angle control system are a sum of two kinds of nose heading angle. One is the ideal nose heading angle ψ_{tan}, which is measured from true north to which the airplane should be directed corresponding to position of the airplane. The other is the nose heading angle ψ_{cmd} which is calculated by the deviation from the target radius R_{cmd} and the actual radius R. The sum of these nose heading angles is converted to roll angle command ϕ_{cmd} through PID parameter. Therefore, the turn radius control system is incorporated as an outer loop of the nose heading angle control system to reduce the turn radius deviation to zero and the roll angle control system is incorporated into the inner loop of the nose heading angle control system as shown in Fig.3.

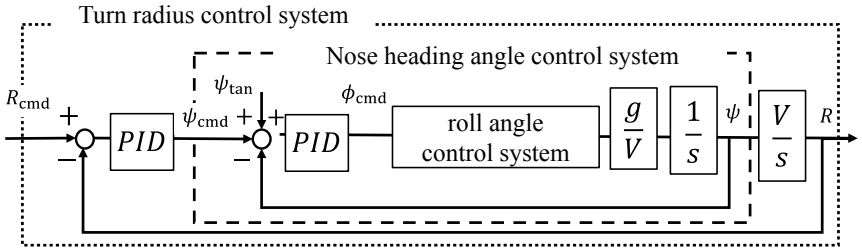

Fig.3 Block diagram of turn path tracking control system.

3-2 Relationship between turning radius deviation and nose heading angle

From Fig.4, after a radius deviation ΔR is defined as a difference between the target turn radius and the actual turn radius, from Fig.4 the relationship between the radius deviation ΔR and the nose heading deviation $\Delta\psi$ measured from the line parallel to the tangent line of the turn circle can be expressed as shown in Eq. (1)

$$\Delta\dot{R} = V_{\mathrm{L}} \sin \Delta\psi \tag{1}$$

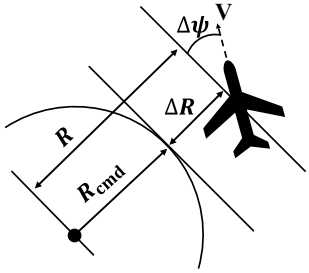

Fig.4 Relationship between turning radius and nose heading angle.

3-3 Derivation of ideal nose heading angle ψ_{tan}

Next, the ideal nose heading angle ψ_{tan} at the current position of the airplane is derived. First, in Fig.5, l_1 is the line connecting the turning center and the current position of the airplane, l_2 is the tangent line at the intersection of l_1 with the target turning path, and l_3 is the line extending to the true north direction from the turning center. The angle between the x-axis and the true north is ε.

The ideal nose heading angle ψ_{tan} is the angle between l_2 and l_3. To obtain the ideal nose heading angle ψ_{tan}, first it is necessary to determine the inclination θ of l_1. The angle θ can be derived from the current position (x_t, y_t) and x coordinates axis with the center of circle as its origin as shown in Eq. (2). Next, the angle λ between the tangent l_2 and the x coordinate axis can be derived as shown in Eq. (3) using the angle θ.

$$\theta = \tan^{-1}\left(\frac{x_0 - x_t}{y_{\mathrm{t}} - y_0}\right) \tag{2}$$

$$\lambda = \theta + \frac{\pi}{2} \tag{3}$$

From the above, the ideal nose heading angle ψ_{tan} can be derived as shown in Eq. (4) using the angle ε between the x coordinate axis and the true north, and the angle λ in Eq. (3).

$$\begin{aligned} \psi_{\tan} &= -(\lambda + \varepsilon) \\ &= -(\theta + \tfrac{\pi}{2} + \varepsilon) \end{aligned} \tag{4}$$

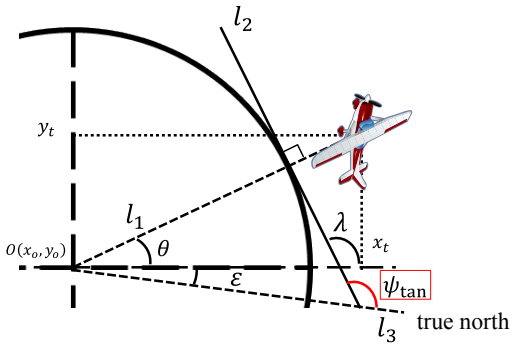

Fig.5　Tangent angle on the target path obtained from the flight position.

4. Simulation

The validity of the proposed turn path tracking control system is evaluated by computer simulations. In simulations, all actual control systems such as velocity control system, altitude control system and the turn path tracking control system are incorporated. All controller in those control systems use PID elements. Also, the feedback rate for simulation is 25 [Hz].

4-1　Controlled airplane

Assuming the flight experiment, data of an actual model airplane are used. The airplane is a low-wing type one and driven by fuel engine and has a mass of about 5.5 kg, a total length of 1.7 m, and a wingspan of about 2 m. The picture of the model airplane is shown in Fig.6.

Fig.6　Model airplane.

4-2　Simulation conditions

At first, the aircraft will fly in a straight line for 50 seconds to keep the airplane stable before entering into a circling flight. In the simulation, the turn radius, the altitude and the air velocity are targeted to be those as shown in Table 1. Besides, the criteria to judge whether the proposed control system works well is set in advance. For the first circle, the deviation of the turn radius is set to within ±14 m, which is 20% of the target radius, by taking into account for the transition such as rise-up and overshoot in control systems. For the final circle, the deviation is set to be ±6 m, taking into account the sensor errors used onboard systems of the actual model airplane. Those errors are specified as standard deviations shown in Table 2.

Simulations were carried out for following three conditions to confirm the convergence of the control system. The first is a no-wind condition. This was conducted to verify the stability of the control system. The second is a steady wind (3 m/s) condition parallel to the x coordinate axis. This was conducted to verify the performance in a disturbing wind environment. The third is the condition that has an initial deviation of 10 meters to confirm the performance of the convergence.

Table 1 Simulation conditions.

Target turning radius	70 m
Target altitude	100 m
Target air velocity	25 m/s

Table 2 Sensor error.

Attitude angle	0.5 deg.
X, Y direction	3 m
Altitude	0.2 m
Velocity	0.17 m/s

4-3 Simulation results

The flight trajectory obtained from the simulation and the time histories of the turning radius are shown below. Also, while the flight trajectory is expressed in three dimensions in Reference 6, it is expressed in two dimensions in this paper to make the trajectory at the time of turning easier to understand.

At first, simulations were carried out under no wind conditions shown in Fig.7. From Fig.7, the maximum turn radius deviation for the first circle was 13.7 m and the radius converged to ±0.6 m in about 24 s from the start of the turn, which was within the target value.

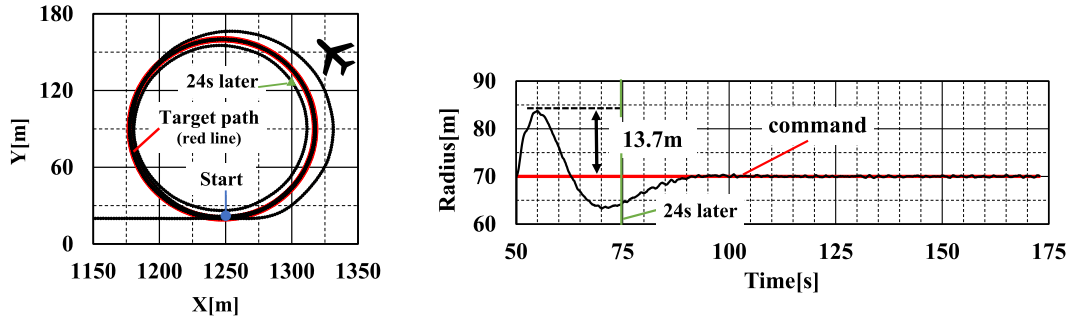

(a) Flight path (b) Time histories of the turning radius

Fig.7 Simulation results (no wind).

Then simulations were carried out for a steady wind of 3 m/s as shown in Fig.8. From Fig.8 the maximum turn radius deviation for the first circle was 12.8 m, and the final deviation was 3.6 m, which was within the target range. It was also confirmed that the radius converged within ±6 m of the target radius in 25 s from the start of the turn.

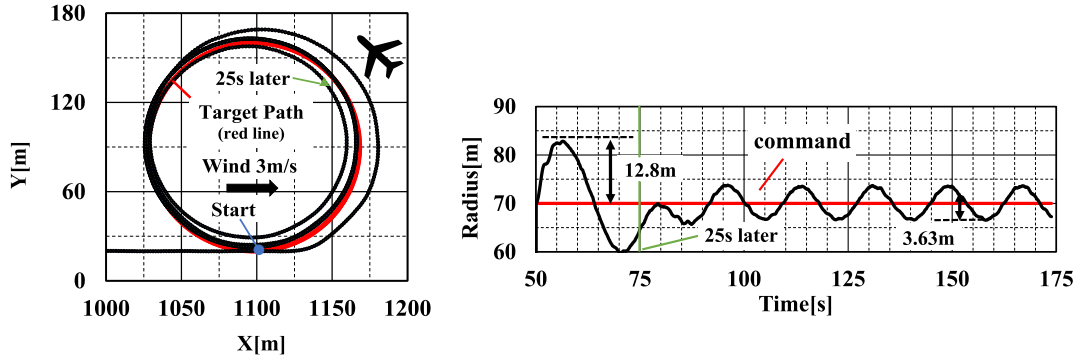

(a) Flight path (b) Time histories of the turning radius

Fig.8 Simulation results (steady wind of 3 m/s).

Finally, the simulation was performed with an initial deviation of 10 m as shown in Fig.9. From Fig.9, it was confirmed that the radius converged within ±6 m of the target radius in 25 s from the start of the turn.

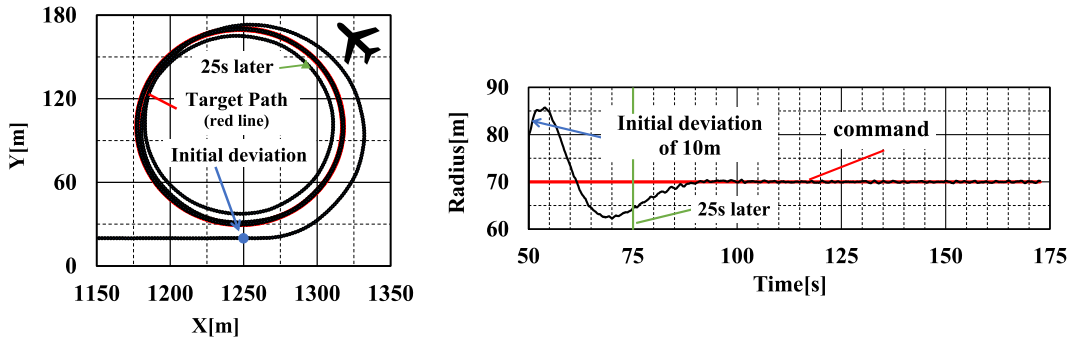

(a) Flight path　　(b) Time histories of the turning radius

Fig.9 Simulation results (initial deviation of 10 m with no wind).

5. Flight verification experiment

A flight verification experiment was conducted using the proposed control system. The target airplane (Fig.6), same as simulation, was mounted with a microcontroller board and an autonomous control program written in C language was executed. Also, the feedback rate is 25 [Hz], the same as simulation. The airplane first follows a straight path and after passing a given point switches to a turning flight to follow a circular path with a radius of 70 m. The airplane then flew to follow a straight path in the opposite direction after completing 5.5 laps of turning flight. The actual flight path results are shown in Fig.10 and the time history of the turning radius is shown in Fig.11. From Fig.10, it can be found that all flight phases follow the target turn path. Fig.11 shows that the turning radius generally follows the command, although there is some vibration around target of 70 m. Also, the average deviation of the radius was 7 m throughout the turn flight. This result was satisfactory considering the sensor error used, control error.

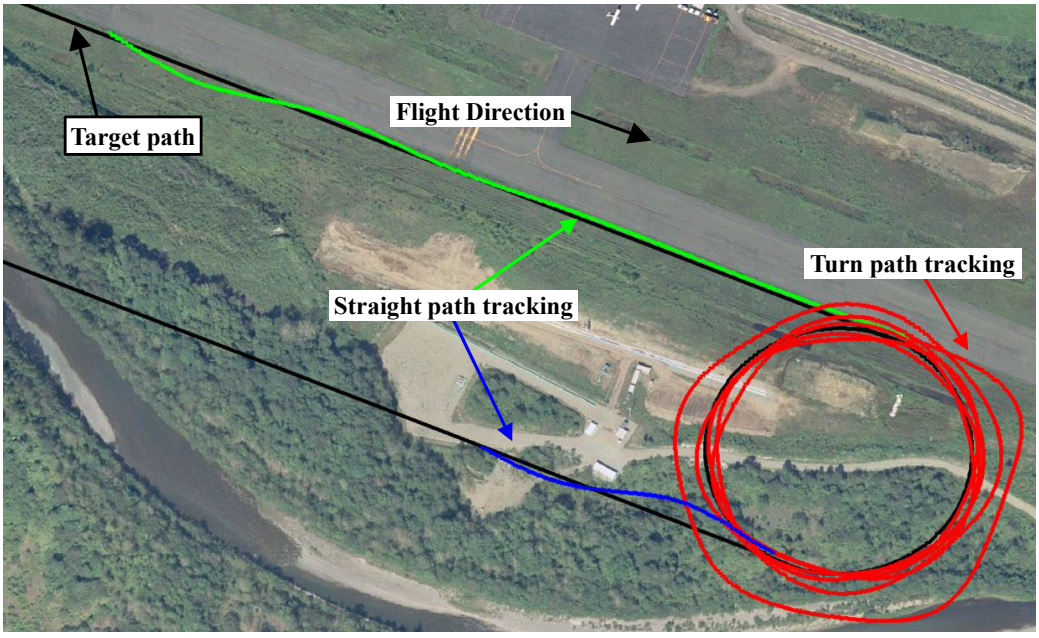

Fig.10 Flight experiment.

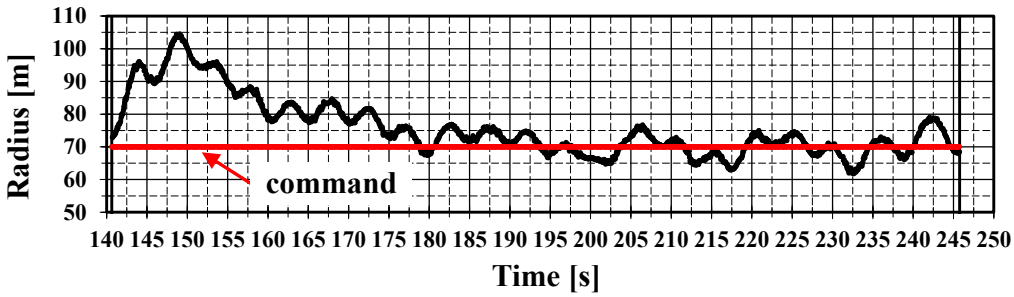

Fig.11 Time history of turning radius.

6. Conclusions

To realize highly accurate turn path tracking, we proposed a new control system to use radius deviation and nose heading angle. The feature of the proposed control system uses two nose heading angles derived from the current position of the airplane and the radius deviation. After simulations, it was confirmed that the airplane could turn within the target deviation against the target turn radius under no wind and a steady wind of 3 m/s.

Finally, flight verification experiment was conducted using the proposed control system, and a stable turn of 5.5 laps was achieved.

Received: December 9, 2024
Accepted: December 20, 2024

References

[1] Hasegawa, K., "Future of Agriculture Using Unmanned Aerial Vehicle", *IIEEJ* vol. 45 No. 4 (2016) pp. 504–507.

[2] Dongwon Jung and Panagiotis Tsiotras, "Bank-to-Turn Control for a Small UAV using Backstepping and Parameter Adaptation", Proceedings of the 17th World Congress The International Federation of Automatic Control Seoul, Korea, July 6-11, 2008.

[3] A. Noonan, D. Schinstock, C. Lewis and B. Spletzer, "Optimal turning path generation for unmanned aerial vehicles", Proceedings of the Ninth IASTED Control and Applications Conference, 2007.

[4] Joshua, M.L., Meyer, N. and Aditya, A. P., "Aggressive Turn-Around Manoeuvres with an Agile Fixed-Wing UAV", *IFAC-PapersOnLine*, vol. 49-17 (2016) pp. 242–247.

[5] Mitomu Shibata, Kakuji Ogawara and Hidenori Shingin, "Skid-to-Turn Maneuver of Small UAV with Side-Force Plate", *Journal of the Japan Society for Aeronautical and Space Sciences*, vol. 64 (2016) pp.317–323.

[6] Kei Yasukawa, Koki Hamazima and Masazumu Ueba, "Turning path tracking control technology for fixed-wing UAV to realize video transmission relay station" *IEICE Communications Express*, Vol.11, No.8, 527–531.

Wataru Miura

Born in 2001, he has been a member of the Department of Production Systems Engineering, Graduate School of Engineering, Muroran Institute of Technology since April 2023. Engaged in study on autonomous flight of Fixed-wing UAV.

一般社団法人 日本 UAS 産業振興協議会（JUIDA）

JUIDA は、日本の無人航空機システム（UAS）の、民生分野における積極的な利活用を推進し、UAS 関係の新たな産業・市場の創造を行うとともに、UAS の健全な発展に寄与することを目的とした中立、非営利法人として、2014 年 7 月に設立されました。

国内外の研究機関、団体、関係企業と広く連携を図り、UAS に関する最新情報を提供するとともに、さまざまな民生分野に最適な UAS を開発できるような支援を行っています。同時に、UAS が安全で、社会的に許容されうる利用を実現するために、操縦技術、機体技術、管理体制、運用ルール等の研究を行うとともに政策提言を行っています。

Technical Journal of Advanced Mobility
次世代移動体技術誌

第 6 号

発行日　：2025 年 1 月 24 日
編集・発行　：一般社団法人日本 UAS 産業振興協議会
東京都文京区本郷 5-33-10
いちご本郷ビル 4F
URL　：https://uas-japan.org/
email　：journal@uas-japan.org

ISSN　2435-5453